Challenging Glass Conference Proceedings – Volume 10 – June 2026 – Louter, Bos & Belis (Eds.)
International Conference on the Architectural and Structural Application of Glass
Challenging Glass Conference 10 – 15-17 June 2026 – TU Delft – The Netherlands

Numerical comparative study on the in-plane seismic behaviour of point-fixed and stick systems

Mir Zafarullah [a], Cella Nicola [a], Chiara Bedon *[a], Pasquale Lucia [b]

a Department of Engineering and Architecture, University of Trieste, Italy, mir.zafarullah@phd.units.it, nicola.cella@phd.units.it, chiara.bedon@dia.units.it
b BLDing Studio STP Srl, Pordenone, Italy, p.lucia@blding.it

Abstract

Major design challenges in facades for multi-story buildings are represented by extreme loading conditions, such as earthquakes. The mechanical response of glass systems, particularly against dynamic loads, is in fact extremely unpredictable, due to a combination of multiple aspects. Even a few details (i.e., connectors) can strongly modify the overall structural performance, in terms of global stiffness, load-bearing capacity, failure mechanisms, etc. Therefore, to accurately detect the true behaviour, performance indicators, and resisting mechanisms of glass against such loads, robust testing protocols and optimized numerical approaches are required. In this study, two different glass facades, namely a Point Fixed Glass Facade (PFGF) and a stick system, are subjected to conventional experimental protocols to numerically explore and compare their mechanical response against in-plane seismic loads. The analysis starts from the preliminary design of the minimum glass thicknesses that are required to sustain the ordinary mechanical loads (wind and self-weight). Under in-plane seismic conditions, as expected, the numerical results show that the two systems behave strongly differently. The response of the stick system is highly influenced by the clearance between the glass panel and the frame, while in the PFGF, discrete fixings play a key role. The PFGF system was found to be more vulnerable to seismic loads than the stick system.

Keywords

Structural glass, Point-fixed glass, Glass facades, Seismic response, Numerical analysis

Article Information

- Digital Object Identifier (DOI): 10.47982/cgc.10.758
- Published by Challenging Glass, on behalf of the author(s), at Stichting OpenAccess.
- Published as part of the peer-reviewed Challenging Glass Conference Proceedings, Volume 10, June 2026, 10.47982/cgc.10
- Editors: Christian Louter, Freek Bos & Jan Belis

1. Introduction

Glass facades have gained more popularity in recent decades due to their lightweight, aesthetic, ease of construction, and energy reduction properties. However, due to the brittle behaviour of glass, facades are extremely susceptible to damage and put human lives at risk under extreme loads such as earthquakes (Bedon et al. 2018).

Historical earthquake data show that seismic actions highly impact the performance of the glass facades (Benuska 1990; Norton et al. 1994; Park et al. 1995). The seismic record from literature also reports severe facade damage during the Northbridge earthquake (1994), the Chile earthquake (2010), and the Christchurch earthquake (2011), even though the primary building structures remained structurally intact (Cella and Bedon 2024a). Such a vulnerability in glass facades stems mainly from the brittle behaviour of glass and the geometrical incompatibility between the deformation of the main structure and the facade components (Fig. 1).

(a) (b) (c)

Fig. 1: Examples of damage in glass facades caused by past earthquakes: (a) Northridge earthquake (1994), (b) Chile earthquake (2010), and (c) Christchurch earthquake (2011) (Baird et al. 2011; Perry et al. 2011).

Among the various types of facade systems, the Point-fixed glass facades (PFGF) and the stick system may exhibit fundamentally different in-plane seismic behaviors when subjected to cyclic lateral loads. The PFGF systems, characterized by discrete mechanical fixings that include bolted spiders, articulation, and steel-based support structure, rely on the translational and rotational capacity of individual connectors to dissipate energy and accommodate in-plane inter-story drift cycles. On the other hand, the stick systems transfer cyclic loads through the aluminum frame, which consists of a mullion-transom grid. The overall response of the system is affected by the clearance between the glass and frame, the behavior of the gaskets, and the position of the setting blocks.

In this context, the present study aims to assess and compare the in-plane seismic response of a PFGF and a stick system through displacement-controlled numerical analyses in ABAQUS. The objective is to characterise the hysteretic behaviour of the two systems and the distribution of stresses in the glass panels in order to compare the seismic vulnerability of the two solutions, thereby providing useful information for a performance-based design of glass facades in seismic regions.

2. Loading protocols

The present study focuses on the numerical analysis of glass facades under in-plane seismic loads. More in detail, it aims to numerically compare and assess the in-plane response of two different facade systems, namely the PFGF and the stick system, starting from the assumption that both were designed in accordance with CNR-DT 210/2013 guideline to serve as the envelope of the same building under the same boundary conditions. To this end, two well-established experimental protocols used to assess the seismic performance of glazed facades are considered in this study. The numerical investigation is performed by applying the crescendo test recommended by AAMA 501.6 (AAMA, 2001) as shown in Fig. 2(a), and a quasi-static test based on FEMA 461, as performed by Aiello et al. (2018) and Cella & Bedon (2024c); see Fig. 2(b).

The crescendo test was introduced by Behr and Belarbi (1996) and consists of four sinusoidal cycles with alternating ramp-up and constant amplitude, with a frequency of 0.8 Hz, and a drift amplitude of ±6 mm for each cycle. The crescendo test was originally intended to be performed on stick systems only; however, in this study, it is also extended to assess the response of the PFGF system. FEMA 461, on the other hand, proposes a controlled displacement test protocol involving repeated cycles with increasing amplitude. Each subsequent step is evaluated at an amplitude equal to 1.4 times that of the previous one.

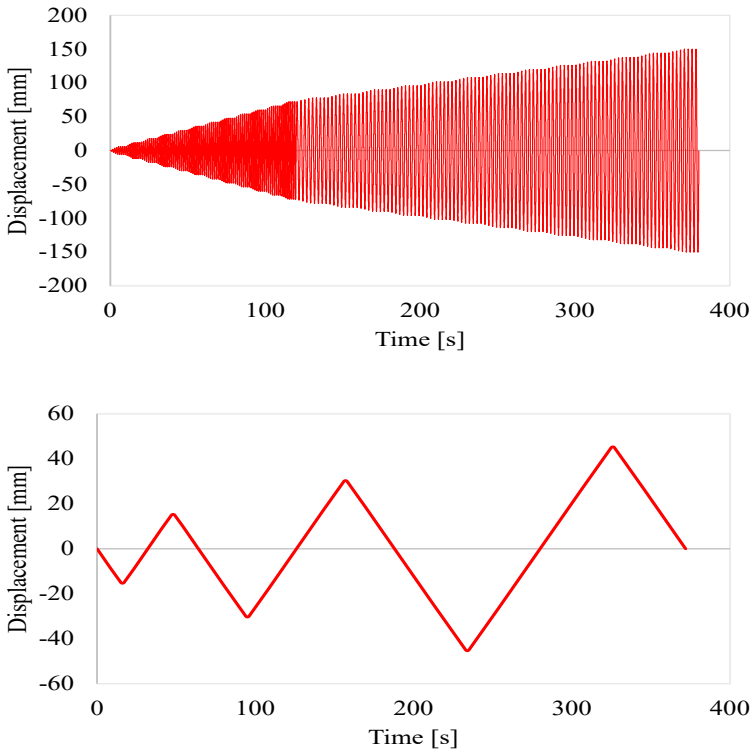

Fig. 2: Reference drift amplitude of (a) crescendo test (AAMA 501.6) and (b) FEMA 461-based quasi-static test as performed by (Aiello et al. 2018) and (Cella & Bedon, 2024c).

3. Examined façade types

There are commonly two types of glass facades, depending on the type of supporting structures, i.e., the stick system and the Point Fixed Glass Facade (PFGF). The stick system façade, as shown in Fig. 3 consists of a continuous metal frame anchored to the floor slabs to support the infill glass panels.

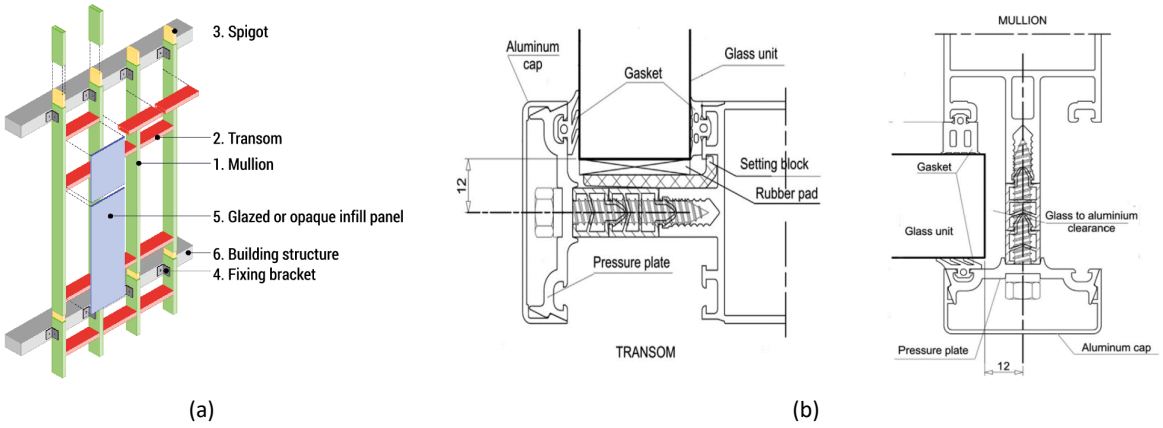

Fig. 3: Examples of (a) stick system (Krawczyk 2020), with (b) details of frame elements and glass connection (Cella and Bedon 2024a).

On the other hand, a PFGF takes advantage of discrete supports only (see Fig. 4). Such a system is generally more expensive than a stick system but provides more transparency. Four-point supported glass panels are the most common types of PFGF (Wei et al. 2013).

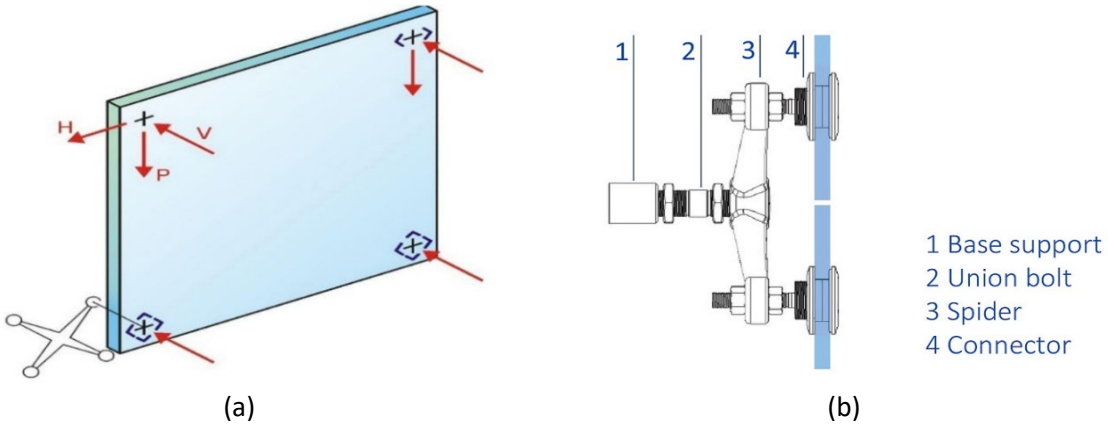

Fig. 4: (a) Schematic representation of boundary conditions for the glass panel and (b) PFGF detailing of supporting components (Inca-Cabrera et al. 2025).

Each system behaves differently due to its support configuration. The mechanical response of a stick system is highly influenced by the clearance between the frame and the glass panel, as well as by the frame inertia and the secondary components. On the other hand, in the PFGF, the glass weight is supported by discrete fixings, and the overall response is highly influenced by the type of spiders used in the system, which connect the glass with the secondary supporting structure. The most popular configuration of the PFGF system includes a spider with slotted holes and bolts with articulation. Such a configuration improves the mechanical performance of the glass facade by allowing controlled rotation (in the order of 7°-8°) and translation (depending upon the washer) of the glass panel. Typical boundary conditions for the glass panel are depicted in Fig. 4 (a).

4. Numerical modelling

4.1. Stick system

To compare the in-plane seismic response of the two systems, they were first designed to withstand the same external loads and to serve as the envelope for the same building, so as to obtain two structurally equivalent systems. In doing so, the inter-story height of the supporting structure and the size of the glass panels were set to 2.80 m and 1990 mm x 1990 mm, respectively. The infill glass panels were assumed to be made of fully tempered laminated glass with a design tensile strength of 83 MPa. For the PFGF, specific reduction factors were considered for the design strength near glass holes. The local design strength was thus estimated as 63 MPa. The glass thickness for each system was calculated using the guidelines provided in the Italian CNR-DT 210/2013. Due to the different boundary conditions, the thickness was calculated as 55.4 (5 mm glass + 4×0.38 mm PVB + 5 mm glass) for the stick system, and 1010.2 (10 mm glass + 2×0.38 mm PVB + 10 mm glass) for the PFGF. The physical properties for the PVB interlayer were selected corresponding to a load scenario with a temperature of 30 °C and a load duration of 30 s.

Moreover, to reduce the computational cost of simulations, only one glass panel was modelled. The laminated glass panel was described using a composite layup shell (S4R elements), defining each layer of the resisting section. Shell elements were also employed to represent the aluminum frame, while the behavior of secondary components such as gaskets and setting blocks, as well as the contact between the frame and the glass, was modelled using Cartesian and Axial connectors. A Hinge connector was also used to model the connection between transoms and mullions. The same numerical strategy was adopted by Cella & Bedon (2024c). The different nonlinear behaviors adopted for the connectors are summarized in Fig. 5 (Cella & Bedon, 2024c), while the physical properties assigned to each material are provided in Table 1. Fig. 6 illustrates the modelling strategy adopted for the stick system.

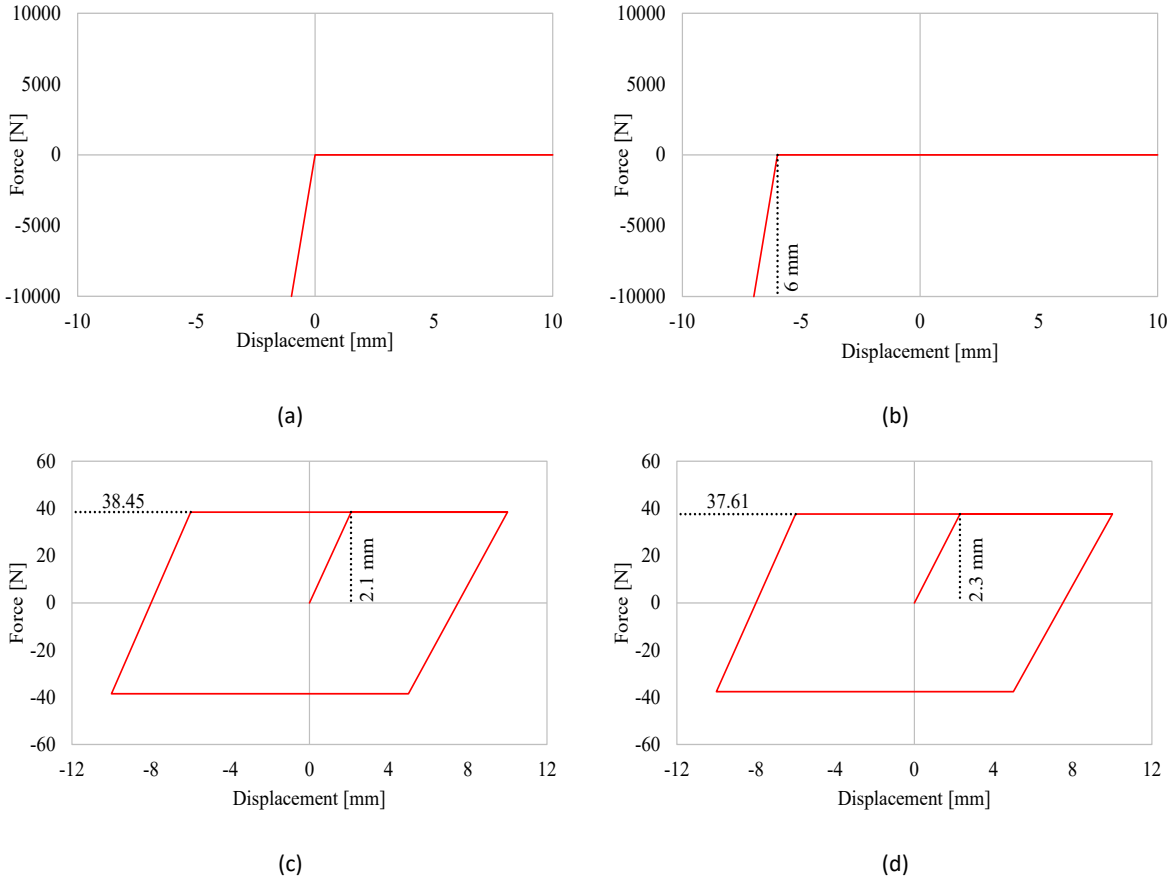

Fig. 5: Nonlinear properties assigned to connectors used to represent: (a) setting block, (b) contact between glass and frame, (c) transom gaskets, and (d) mullion gaskets.

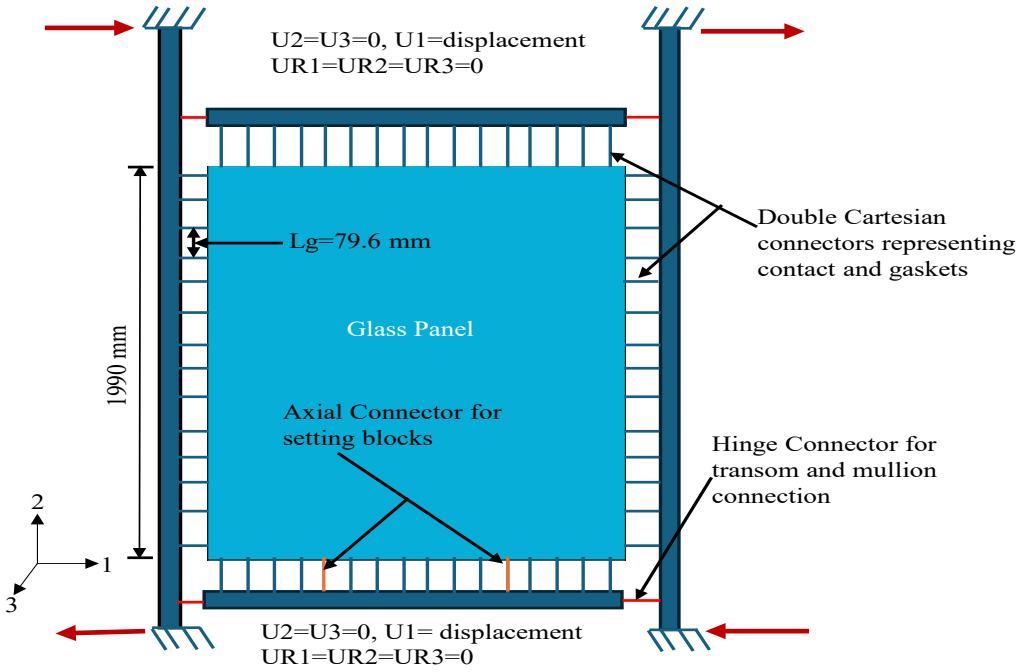

Fig. 6: Graphical representation of the numerical modelling strategy adopted for the stick system.

4.2. PFGF system

For analysing the seismic response of the PFGF system, see Fig. 7, the glass was modelled using shell elements with a composite layup, the supporting structure (steel columns) was replicated with 1D beam elements, and the behaviour of other components (including spider arm, bolt head, and articulation) was modelled using connector elements, as described by Hosseini et al. (2026). In detail, the fixing part of the spider connections was modelled using 1D beam elements, while a combination of Cartesian+Align and Join+Rotation connectors was used to model the spider arms and the articulation behaviour, respectively.

Both systems were subjected to the same loading and boundary conditions (see Fig. 6 and Fig. 7). The mesh size for the glass panel was set to 100 mm for both systems; however, to accurately capture the results in the PFGF, the mesh size was reduced to 4 mm around the holes.

Table 1: Material properties.

Material	Density (kg/m^3)	E (MPa)	ν (-)	σ_y (MPa)	σ_u (MPa)	ε_u (-)
Glass	2500	70000	0.23	-	-	-
PVB	1100	2.4	0.49	-	-	-
Aluminum	2700	70000	0.30	120	172.78	0.109
Stainless Steel	7850	202040	0.30	208.37	757.01	0.360
S355 Steel	7850	202470	0.30	427.19	590.20	0.089

E: Modulus of Elasticity; ν: Poisson's ratio; σ_y = Yielding stress; σ_u: Ultimate stress; ε_u: Ultimate strain

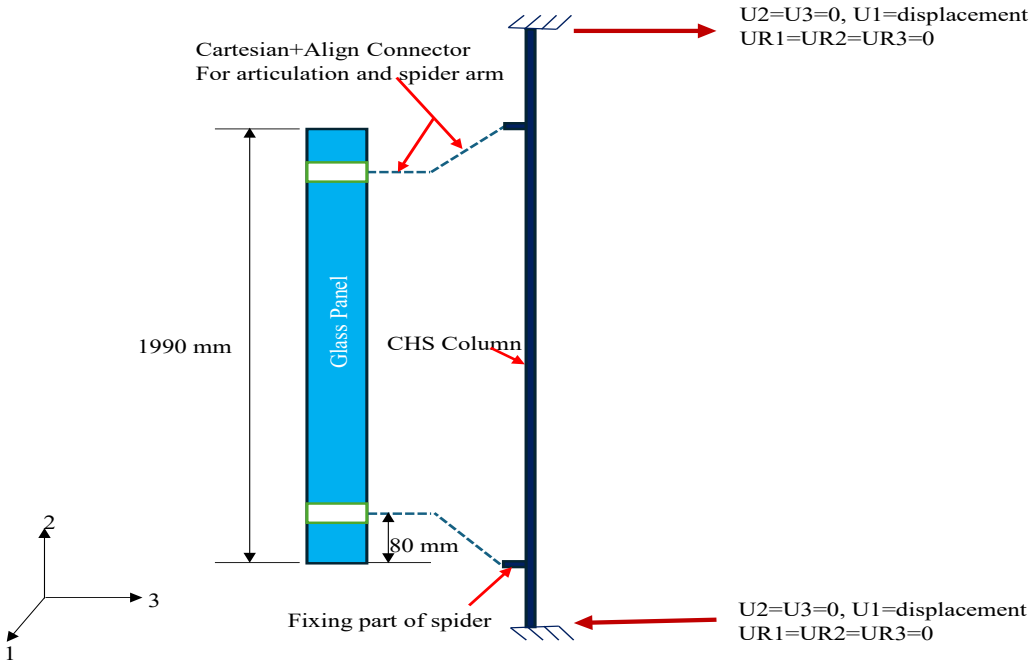

Fig. 7: Graphical representation of the numerical modelling strategy adopted for the PFGF system.

5. Numerical results

5.1. Quasi-static test

Fig. 8 shows a comparison between the stress distributions observed in the PFGF and stick system at the maximum imposed displacement of 45 mm. Both systems exhibit a maximum stress of approximately 10-11 MPa at the edges due to contact with the supporting structure, i.e., the frame for the stick system and the local fixings for the PFGF.

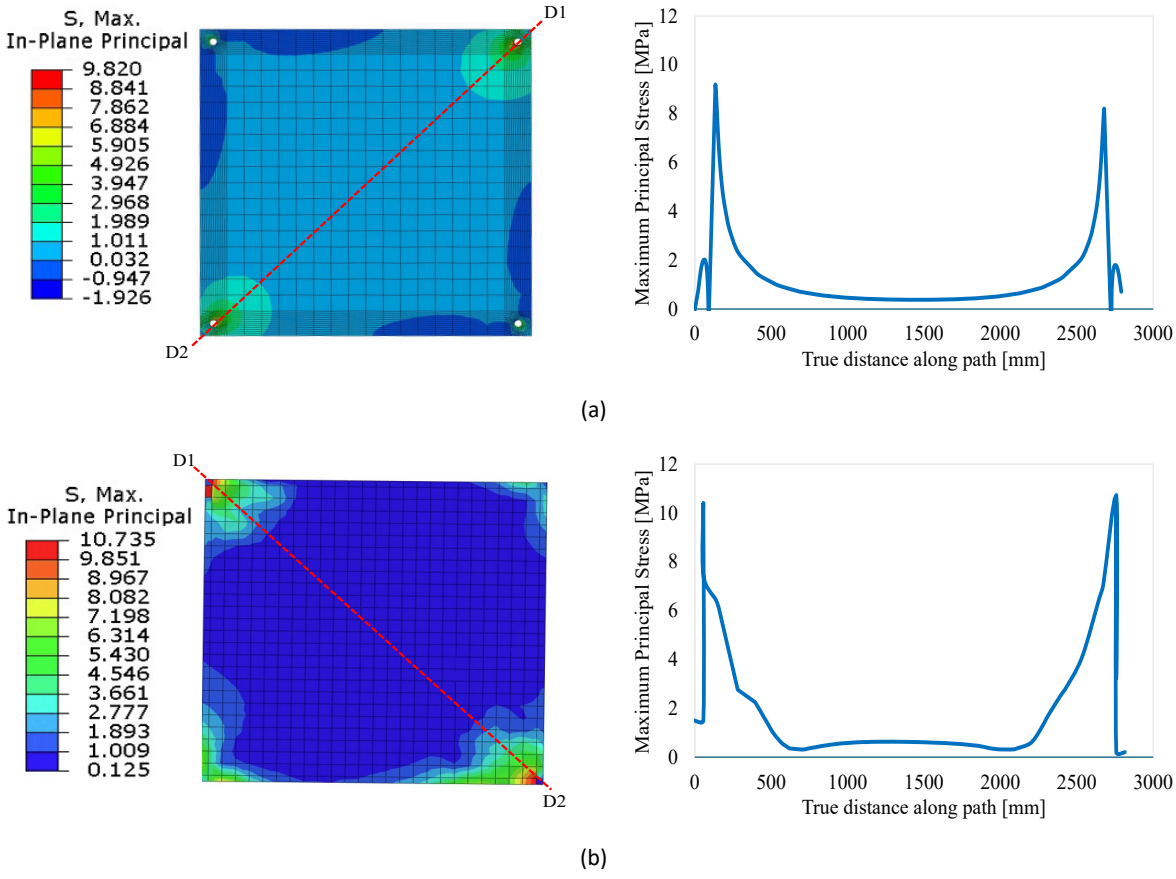

Fig. 8: In-plane principal stress distribution at the maximum imposed displacement for (a) PFGF and (b) stick system (values in MPa).

The hysteresis loops for the PFGF and stick system, as shown in Fig. 9, reveal major differences in terms of structural behaviour.

The force-displacement curve for the PFGF system, see Fig. 9(a), exhibits wider hysteretic loops, which is a key indication of an energy-dissipating system. Furthermore, the system exhibits linear behaviour during the first few cycles, with relatively high stiffness (up to 30 mm). Subsequently, a reduction in stiffness is observed as displacement increases, which is due to the closing of the gap between the bolt and the glass. At this point, the bolt begins to bear the load, and the spherical washer rotates progressively, altering the geometry of the load path and causing a reduction in lateral stiffness.

On the other hand, the force-displacement curve for the stick system, as shown in Fig. 9(b), is essentially a single thin S-shaped line with a narrower loop area, which suggests a negligible energy dissipation. The results also highlight an increase in stiffness following a displacement of approximately 20 mm. Initially, the response is governed by the stiffness of the frame and the behaviour of the gaskets.

The glass then comes into contact with the frame and begins to act as a diagonal compression strut. This mechanism results in an increase in stiffness in the force-displacement response.

Overall, the results show that the two systems respond differently to the quasi-static loading protocol: the PFGF system exhibits greater overall stiffness and energy dissipation than the stick system.

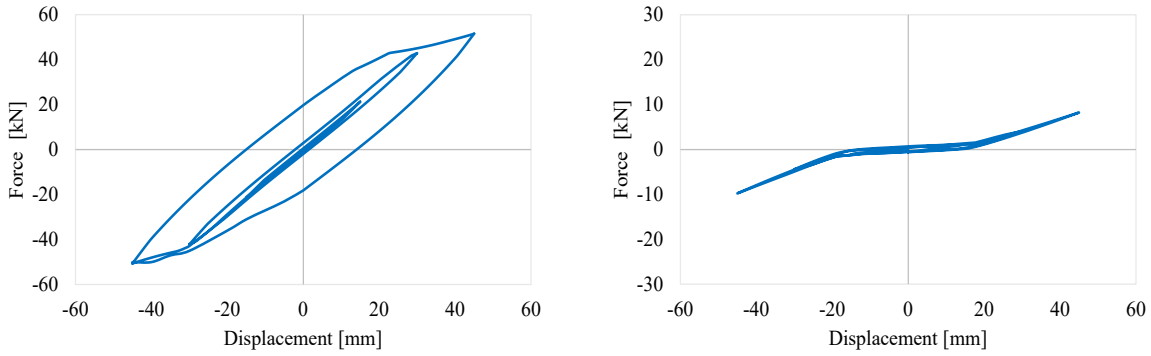

(a) (b)

Fig. 9: Cyclic force-displacement response under quasi-static loading for (a) PFGF and (b) stick system.

5.2. Crescendo test

The numerical analysis of the two-system using the crescendo test revealed that the PFGF reached its design tensile strength during the first phase of the crescendo test, which corresponds to high loading frequency and low displacement amplitudes. On the contrary, the stick system reached its design strength in the second phase of the crescendo test, which is characterized by a lower loading frequency and large displacement amplitudes. This suggests that the PFGF performs poorly under high-frequency loading, while the stick system is more susceptible to failure under large displacements, irrespective of loading frequency.

In detail, Fig. 10 shows a comparison between the maximum stress observed in the PFGF and the stick system against the imposed in-plane displacement. The results show that the PFGF reaches its maximum design strength at 27 mm, while the stick system exceeded its design strength at 62 mm. This comparison reveals that the glass in the PFGF system is more vulnerable compared to that in the stick system in the presence of seismic loads. Furthermore, the maximum in-plane stress in the glass for the PFGF system remained below 10 MPa even at ±45 mm displacement under quasi-static loading; however, it sharply exceeded design strength (83 MPa) at only ±27 mm under the crescendo dynamic test, clearly reflecting the severe impact of dynamic forces on the system.

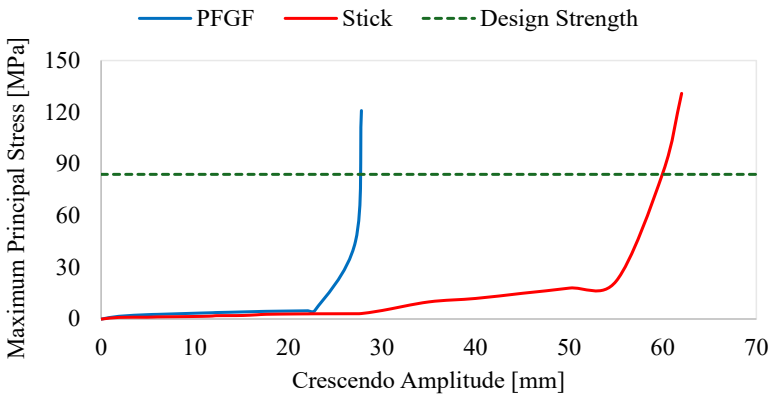

Fig. 10: Maximum stress in the PFGF and stick system as a function of the imposed displacement.

Furthermore, Fig. 11 represents the contour plots for stress distributions in the PFGF and stick system after the strength of the glass has been exceeded.

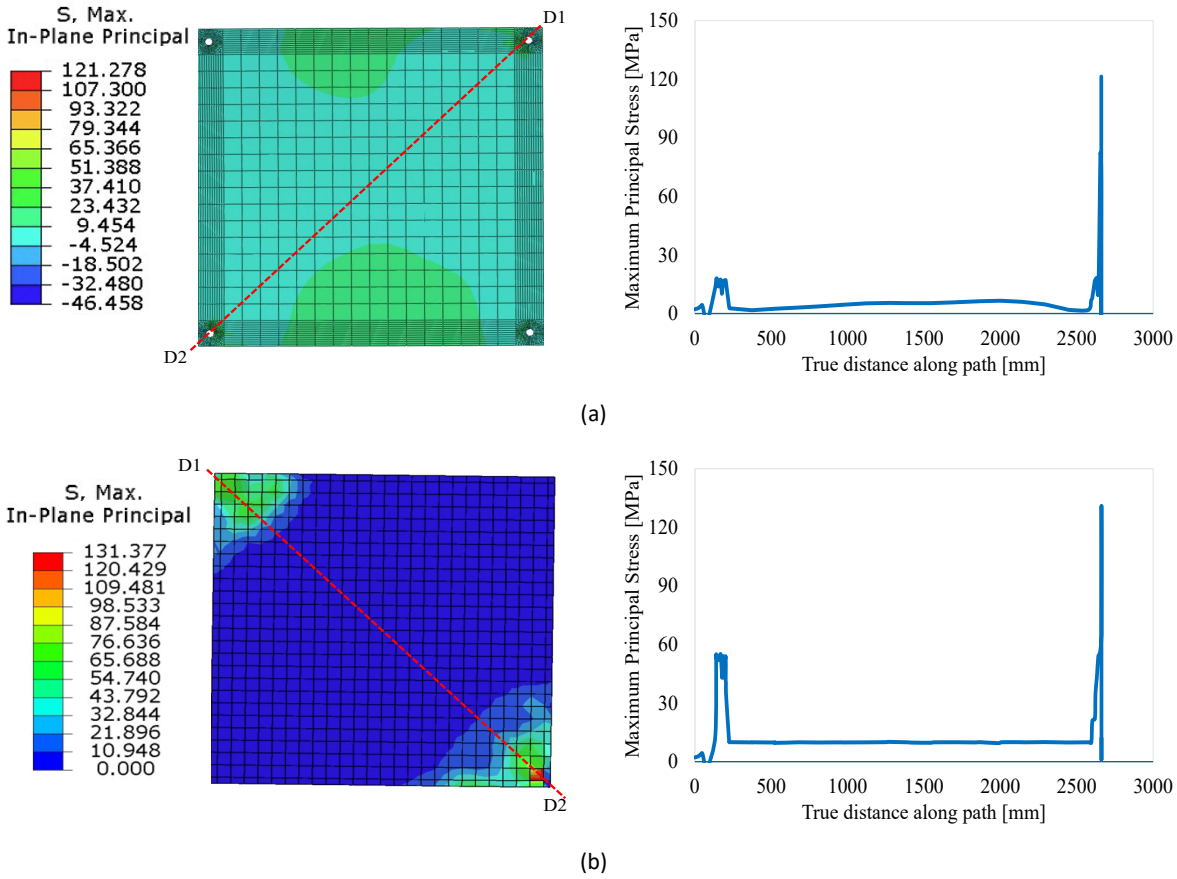

Fig. 11: In-plane principal stress distribution at the imposed displacement corresponding to the first exceedance of the design strength for (a) PFGF and (b) stick system (values in MPa).

Fig. 11(a) shows that high local stress can be induced in the PFGF around its holes even with a relatively small in-plane displacement (27 mm). This is due to the limited clearance (2.5 mm) between the glass and the fixing. Furthermore, the load is transferred via small contact areas, resulting in high stresses at the holes. This does not occur in the stick system, where the clearance between the glass and the frame is greater (6 mm), and the load is transferred across a wider contact surface.

Additionally, the force-displacement curves from the crescendo test, shown in Fig. 12, also highlights some discrepancies in the overall response of the two systems.

The PFGF exhibited substantially wider hysteresis loops beyond ±30 mm displacement amplitude during the quasi-static loading protocol; however, the widening of the curve for the same system can be observed at the earlier stages during the crescendo test (see Fig. 12(a)). In detail, the wider hysteresis loops observed in the quasi-static test were attributed to the large displacement amplitudes up to ±45 mm, which exceeded the linear response threshold of approximately ±30 mm. Similarly, the crescendo test was conducted at displacement amplitudes lower than this threshold (27 mm, where glass reaches its design strength), resulting in comparatively narrower loops consistent with the linear elastic regime identified in the quasi-static test. However, a slight widening of hysteresis loops can be observed in the system beyond ±27 mm displacement in the crescendo test Fig. 12(a), which is notably earlier than the ±30 mm threshold recorded under quasi-static loading conditions. This earlier onset of loop widening is due to dynamic excitation in the crescendo test, which suggests that the system exhibits more vulnerability to dynamic forces. Accordingly, this phenomenon reflects that not only displacement amplitude, but also dynamic loading accelerates the activation of nonlinear mechanisms within the system. This means that dynamic forces push the PFGF system to exceed its linear limit much earlier than expected. Thus, the crescendo test reveals the sensitivity of the PFGF system to dynamic excitations that a quasi-static test alone could not capture.

In addition, the result for the PFGF system, as shown in Fig. 12(a), demonstrates that along the primary loading and unloading paths, the PFGF system exhibits a consistent and essentially constant stiffness (1.4 kN/mm) with minor cycle-to-cycle variation. In addition, the system achieves a peak force of ±40 kN corresponding to the ±27 mm displacement and recovers its shape fully upon unloading at initial stages. This suggests that no permanent drift or residual displacement has been experienced by the system.

In contrast, the force-displacement curve for the stick system, shown in Fig. 12(b) confirms that the stick system can accommodate larger displacements. Nevertheless, the system shows low initial stiffness at ±20 mm displacement; such lower initial stiffness in the system can be associated with the gap (6 mm) between the frame and the glass. In addition, at this level of imposed displacement, the force-displacement curve is mainly governed by the behavior of gaskets. However, after about ±20 mm, the system experiences a rise in its stiffness. This rise is primarily associated with the gap closure when the glass and frame come in contact. An increase from an initial stiffness of 0.09 kN/mm to 0.30 kN/mm can also be observed in the system. Furthermore, Fig. 12 also depicts that the system exhibits negligible energy dissipation, which is evidenced by its narrower loops.

Overall, the PFGF exhibits approximately four times more lateral stiffness (1.4 kN/mm) than the stick system (0.30 kN/mm). Conversely, the latter accommodates larger displacements (up to ±62 mm) due to the clearance between glass and frame. The PFGF system produces elliptical hysteresis loops due to dynamic loading conditions, indicating considerable energy dissipation, however, at the cost of high stress in the glass panel. While the stick system with zero enclosed area shows negligible energy dissipation. The PFGF system represents almost constant stiffness with small degradation over successive loading cycles, while the stick system shows a meaningful rise in stiffness.

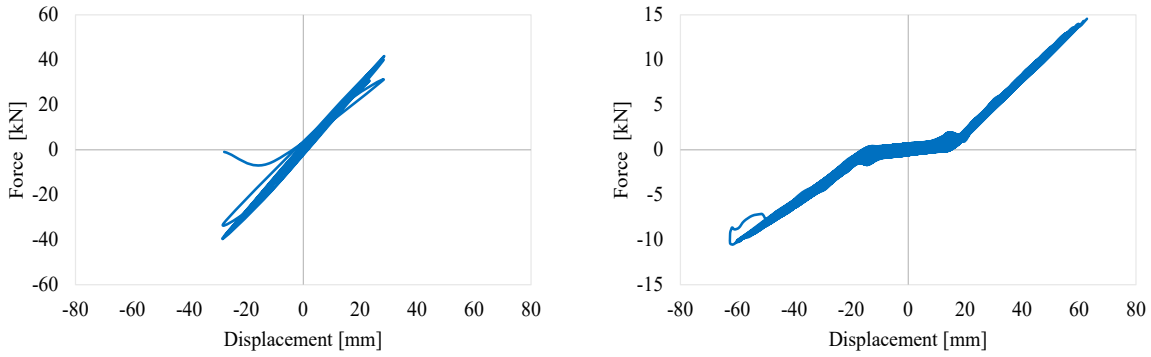

(a) (b)

Fig. 12: Cyclic force-displacement response under crescendo test for (a) PFGF and (b) stick system.

6. Conclusions

Point-Fixed Glass Facades (PFGFs) and stick systems are among the most used systems in the construction of curtain walls. Since glass is a brittle material, facade systems need specific tools for a safe and optimized design.

In this study, attention was given to the numerical comparison of the in-plane seismic response of the PFGF and stick system. To do this, both systems were subjected to a quasi-static cyclic test and the crescendo test. The numerical results revealed a markedly different response of the two systems, primarily influenced by the support configuration of the glass panel.

In detail, the stick system demonstrated a greater capacity to accommodate large in-plane displacements than the PFGF thanks to the clearance and a larger contact between the glass and the frame, which allows for a better distribution of stresses on the glass panel. On the other hand, the PFGF achieved a higher ultimate load and dissipated more energy. In other terms, the PFGF exhibited approximately four times more lateral stiffness than the stick system.

In conclusion, a PFGF is more vulnerable – in terms of glass breakage – compared to a stick system when subjected to in-plane seismic forces. This finding highlights the need to carefully consider the choice of the facade system, particularly in earthquake-prone regions.

Acknowledgements

This research investigation was carried out in the framework of an Italian Recovery and Resilience Plan (PNRR) research project about the “Analysis and design of multifunctional and structurally efficient glass facades,” carried out at the University of Trieste—Department of Engineering and Architecture (Italy). The publication content has been produced with co-funding from the European Union—Next Generation EU.

References

AAMA. (2001). Recommended dynamic test method for determining the seismic drift causing glass fallout from a wall system. Publication No. AAMA, 501.

Aiello, C., Caterino, N., Maddaloni, G., Bonati, A., Franco, A., & Occhiuzzi, A. (2018). Experimental and numerical investigation of cyclic response of a glass curtain wall for seismic performance assessment. Construction and Building Materials, 187. https://doi.org/10.1016/j.conbuildmat.2018.07.237

Anna Krawczyk. (2020). Sustainable buildings – development of low energy and eco-friendly constructions. https://doi.org/10.24427/978-83-67185-24-0_6

Bedon, C., Zhang, X., Santos, F., Honfi, D., Kozłowski, M., Arrigoni, M., Figuli, L., & Lange, D. (2018). Performance of structural glass facades under extreme loads – Design methods, existing research, current issues and trends. In Construction and Building Materials (Vol. 163). https://doi.org/10.1016/j.conbuildmat.2017.12.153

Behr, R. A., & Belarbi, A. (1996). Seismic test methods for architectural glazing systems. Earthquake Spectra, 12(1). https://doi.org/10.1193/1.1585871

Behr, R. A., Belarbi, A., & Brown, A. T. (1995). Seismic Performance of Architectural Glass in a Storefront Wall System. Earthquake Spectra, 11(3). https://doi.org/10.1193/1.1585819

Benuska, K. L. (1990). Ground motion, Loma Prieta earthquake reconnaissance report. Earthquake Spectra, 6.

Bianchi, S., & Pampanin, S. (2022). Fragility Functions for Architectural Nonstructural Components. Journal of Structural Engineering, 148(10). https://doi.org/10.1061/(asce)st.1943-541x.0003352

Cella, N., & Bedon, C. (2024a). Numerical modelling of global/local mechanisms and sensitivity analysis for the seismic vulnerability assessment of glass curtain walls. Engineering Structures, 319. https://doi.org/10.1016/j.engstruct.2024.118859

Cella, N., & Bedon, C. (2024b). Numerical Seismic Fragility Analysis of Glass Curtain Walls: Gaps and Challenges in Modelling Optimization and Limit Performance Indicators. Buildings, 14(12). https://doi.org/10.3390/buildings14123863

Cella, N., & Bedon, C. (2024c). Numerical Seismic Fragility Analysis of Glass Curtain Walls: Gaps and Challenges in Modelling Optimization and Limit Performance Indicators. Buildings, 14(12). https://doi.org/10.3390/buildings14123863

CNR-DT 210/2013. (n.d.). NATIONAL RESEARCH COUNCIL OF ITALY ADVISORY COMMITTEE ON TECHNICAL RECOMMENDATIONS FOR CONSTRUCTION Guide for the Design, Construction and Control of Buildings with Structural Glass Elements.

Cowan, H., Beattie, G., Hill, K., Evans, N., McGhie, C., Gibson, G., Lawrance, G., Hamilton, J., Allan, P., Bryant, M., Davis, M., Hyland, C., Oyarzo-Vera, C., Quintana-Gallo, P., & Smith, P. (2011). The M8.8 Chile earthquake, 27 february 2010. Bulletin of the New Zealand Society for Earthquake Engineering, 44(3). https://doi.org/10.5459/bnzsee.44.3.123-166

(FEMA), F. E. M. A. (2007). Interim Protocols For Determining Seismic Performance Characteristics of Structural and Nonstructural Components Through Laboratory Testing. In FEMA 461 (Number June).

Hosseini, S. A., Jordão, S., Rebelo, C., Bedon, C., Inca Cabrera, E., & Rahnavard, R. (2026). Cyclic behaviour of point fixed glass façade systems: Benchmark model. Structures, 87, 111621. https://doi.org/10.1016/j.istruc.2026.111621

Inca-Cabrera, E., Jordão, S., Rebelo, C., Bedon, C., Mesquita, A., & Hosseini, S.-A. (2025). Experimental and numerical investigation of in-plane cyclic response of a point-fixed glass façade system for seismic performance assessment. Journal of Building Engineering, 108, 112956. https://doi.org/10.1016/j.jobe.2025.112956

Norton, J. A., King, A. B., Bull, D. K., Chapman, H. E., McVerry, G. H., Larkin, T. J., & Spring, K. C. (1994). Northridge earthquake reconnaissance report. Bulletin of the New Zealand Society for Earthquake Engineering, 27(4). https://doi.org/10.5459/bnzsee.27.4.235-344

Park, R., Billings, I. J., Clifton, G. C., Cousins, J., Filiatrault, A., Jennings, D. N., Jones, L. C. P., Perrin, N. D., Rooney, S. L., Sinclair, J., Spurr, D. D., Tanaka, H., & Walker, G. (1995). The Hyogo-Ken Nanbu earthquake (the Great Hanshin Earthquake) of 17 January 1995. Bulletin of the New Zealand Society for Earthquake Engineering, 28(1). https://doi.org/10.5459/bnzsee.28.1.1-98

Wei, Y., Chen, S., & Au, F. T. K. (2013). Failure analysis of four-point-supported glass panels subjected to blast loading. HKIE Transactions Hong Kong Institution of Engineers, 20(1). https://doi.org/10.1080/1023697X.2013.785089Zito, M., Nascimbene, R., Dubini, P., D'Angela, D., & Magliulo, G. (2022). Experimental Seismic Assessment of Nonstructural Elements: Testing Protocols and Novel Perspectives. In Buildings (Vol. 12, Number 11). https://doi.org/10.3390/buildings12111871

Challenging Glass Conference Proceedings – Volume 10 – June 2026 – Louter, Bos & Belis (Eds.)
International Conference on the Architectural and Structural Application of Glass
Challenging Glass Conference 10 – 15-17 June 2026 – TU Delft – The Netherlands

Platinum Sponsor

SAINT-GOBAIN

Gold Sponsors

EASTMAN

kuraray

NorthGlass®

sedak

seele

Silver Sponsors

DOW®

octatube

PERMASTEELISA GROUP

SEEN

Organisation

TU Delft

Technische Universität München

GHENT UNIVERSITY